Numerical Simulation of the Single-Stage Depressed Collector for the 2 MW, CW, 170 GHz Coaxial Cavity Gyrotron

S. Illy[1], B. Piosczyk[1], S. Raff[2]

[1]Institut für Hochleistungsimpuls- und Mikrowellentechnik (IHM),
[2]Institut für Reaktorsicherheit (IRS)
Forschungszentrum Karlsruhe, Association EURATOM-FZK,
Hermann-von-Helmholtz-Platz 1, D-76344 Eggenstein-Leopoldshafen, Germany

Abstract

A 2 MW, CW, 170 GHz coaxial cavity gyrotron as could be used for ITER is under development in cooperation between CRPP Lausanne, FZK Karlsruhe, HUT Helsinki and Thales Electron Devices. The gyrotron requires a collector which is capable to dissipate a power of up to 3 MW of the exhausted electron beam. A collector design with sweeping coils placed inside the hollow electron beam had to be discarded. This became necessary because of the eddy currents induced mainly in the outer collector walls which strongly modify the distribution of the sweeping magnetic field. Therefore a design with an inner static collector coil and an outer sweeping coil is under consideration.

1 Introduction

Millimeter waves can be used with great advantage for heating magnetically confined plasmas of thermonuclear fusion devices as well as for controlling plasma instabilities. They have been applied successfully in different fusion experiments [1]. At present gyrotrons with an RF output power of 1 MW, CW at 140 GHz are close to become state of the art [2]. For fusion experiments of the next generation such as the International Thermonuclear Experimental Reactor (ITER), it is estimated that microwave power of at least 24 MW, CW at 170 GHz will be needed [3]. By increasing the output power per unit to 2 MW, the costs of the installations of the electron cyclotron wave (ECW) systems could be reduced, and in addition the upper port launcher could be made more compact. As has been demonstrated experimentally coaxial cavity gyrotrons have the potential to fulfil this requirement [4]. Therefore the development of an industrial prototype of a coaxial cavity gyrotron with an RF output power of 2 MW, CW at 170 GHz is in progress in cooperation between European Associations (CRPP Lausanne, FZK Karlsruhe and HUT Helsinki) together with European tube industry (Thales Electron Devices, Velizy, France). The main nominal parameters of the gyrotron are summarized in Tab. 1.

2 Design of the gyrotron collector

2.1 General considerations

In gyrotrons the electron beam is guided by a cylindrical symmetric magnetic field. As a consequence of Busch's

cavity mode	$TE_{34,19}$
frequency	170 GHz
RF output power	2 MW
beam current	75 A
accelerating voltage	90 kV
retarding voltage	≈ -34 kV
output efficiency	$\geq 45\%$
cavity magnetic field	6.87 T
beam radius in cavity	10.0 mm

Table 1: Nominal design parameters of the 170 GHz, 2 MW, CW coaxial cavity gyrotron.

theorem [5] the guiding centers of the electron beam trajectories follow with high accuracy a path along a constant magnetic flux surface with the enclosed flux Φ_b independently of the electron energy:

$$\Phi_b = \pi \int_0^{R_b(z)} B_z(z,r) r dr \cong \pi R_{\mathrm{bcav}}^2 B_{\mathrm{cav}} \cong \mathrm{const} \quad (1)$$

$B_z(z,r)$ is the axial component of the magnetic field. R_{bcav} and B_{cav} are the beam radius and the magnetic field value at $z = z_{\mathrm{cav}}$, the position of the cavity.

The Busch's theorem determines as well the radius R_b and the radial width ΔR_b of the hollow electron beam of a gyrotron. In the case of coils placed outside the hollow electron beam, R_{bcoll} and $\Delta R_{\mathrm{bcoll}}$ are given approximately by (paraxial approximation):

$$R_{\mathrm{bcoll}} \cong R_{\mathrm{bcav}} \times \sqrt{B_{\mathrm{cav}}/B_{\mathrm{coll}}}, \quad (2)$$

$$\mathrm{and} \quad \Delta R_{\mathrm{bcoll}} \cong \Delta R_{\mathrm{bcav}} \times \sqrt{B_{\mathrm{cav}}/B_{\mathrm{coll}}}. \quad (3)$$

The subscripts 'cav' and 'coll' are used to characterize quantities inside the cavity and the collector, respectively.

In general, the stray field of a SC-magnet changes sufficiently slowly to ensure an adiabatic motion of the electron beam [5]. In this case the transverse momentum $p_\perp$ of the electrons decreases with the magnetic field as $p_\perp \propto \sqrt{B(z)}$. The radial width of the beam varies approximately as given in eq. 3. Thus, for a collector with a given radius R_{bcoll} the instantaneous peak power density at the collector surface can only be modified by a variation of the axial dissipation width ΔL_{coll} given approximately by: $\Delta L_{\text{coll}} \cong \Delta R_{\text{bcoll}} / \sin(\phi_{\text{coll}})$ with the incident angle ϕ_{coll} between the beam and the collector surface. The radial beam width ΔR_{bcoll} inside the collector can be increased due to non adiabatic effects along the beam path by up to twice the Larmor radius $R_L \propto 1/B_{\text{coll}}$. Because of the low value of B_{coll} the beam width inside the collector may increase significantly resulting in a decrease of the instantaneous surface power density.

2.2 Design constrains

The interaction of the electron beam with the RF field inside the cavity results in a strong energy dispersion. The energy distribution after the interaction as shown in Fig. 1 has been obtained from a self consistent code for the nominal parameters. This distribution has been taken for the design calculations of the collector. In order to increase the overall efficiency of the gyrotron and to decrease the power to be dissipated, a single-stage depressed collectors (SDC) with a retarding collector potential of about 34 kV will be used. Taking the reduction of the remaining beam power due to the deceleration of the electrons into account, still about 2.3 MW has to be handled at the collector walls for the 2 MW coaxial gyrotron at nominal conditions. This power increases to about 3 MW (time averaged) if the RF output power of the gyrotron will be fast modulated (up to 5 kHz) between about 0.5 and 2 MW by variation of the body voltage as required by the users.

The goal of the collector design was to keep the time averaged power density within $p_{\text{ave}} \leq 500 \, \text{W/cm}^2$. The instantaneous peak power density and the sweeping rate should limit the maximum temperature oscillation $\Delta T_{\text{peak}} < 100 \, ^\circ\text{C}$ in order to keep the thermo mechanical stresses low. In order to keep p_{ave} within the required limits a sweeping of the electron beam along the collector surface due to time-varying magnetic fields produced by additional collector coils is needed. The sweeping rate is limited by the diffusion time of the magnetic field related to the eddy currents induced in the metallic walls and described by the skin effect. The temperature rise ΔT_{max} of the surface of a copper wall depends on the
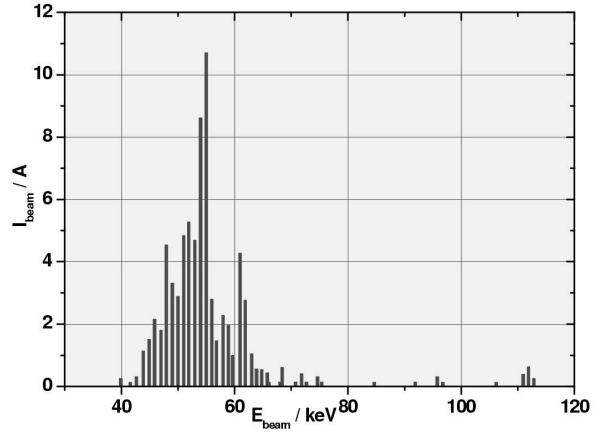
Figure 1: Energy dispersion of the electron beam after RF-interaction as taken for the design calculations.
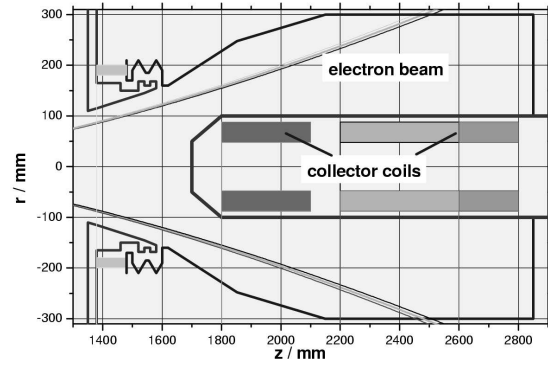
Figure 2: Schematic view of the considered collector geometry.

power density and the applied time τ according to [6]:

$$\Delta T_{max} \cong 0.31 \times p_{\text{wall}}(\text{W/cm}^2) \times \sqrt{\tau/\text{s}}. \qquad (4)$$

The thickness has been assumed to be large compared to the heat diffusion length $\delta_{1/e} \cong 15 \times \sqrt{\tau/\text{s}}$ (for copper).

A schematic view of the investigated collector geometry is given in Fig. 2. The coaxial insert contains the collector coils which has been thought to be used both for shaping the static magnetic field distribution and for performing the beam sweeping along the collector wall.

3 Numerical collector simulation

3.1 The simulation code

The program **ESRAY** used to calculate the power density on the collector wall was developed at FZK/IHM. It is a 2.5-dimensional self-consistent electrostatic ray-tracing code containing the following features:

- The electric field is calculated on a structured non-orthogonal mesh using a fast iterative multi-grid solver. The contribution of the space charge of the electron beam is taken into account.

- The magnetic field created by the main solenoids and the collector solenoids is calculated by numerical integration on the same mesh points. This method is only valid in the stationary case and can not take into account the contribution of eddy currents induced by varying magnetic fields.

  To include these time-dependent effects in the numerical computation, it is possible to import magnetic field distributions calculated by the commercial **ANSYS** Finite Element Code.

- After interpolation of the electric and magnetic field components to the particle positions, the particles are pushed using Boris' algorithm, an energy conserving leapfrog-scheme. Two spatial components (z and r) and all three velocity components are taken into account. Only a small number (50-200) of particles is used and a "trace" of the particles is stored while the particles pass the computational domain.

  This trace gives the charge densitiy of the electron beam that is used as new input for the potential solver.

- About 10–20 iterations are needed to reach a self-consistent solution.

- The wall loading due to the dissipated beam is evaluated from the electron trajectories. The calculation of trajectories of secondary electrons emitted on the collector walls and their corresponding wall loading is under development and will be finished in near future.

3.2 Simulation set-up and results

All simulations were performed on a simulation grid of 160×36 grid cells (indicated in Fig. 3, where only every 4th grid line is shown). A retarding potential of 35 kV was applied in all calculations. The spent electron beam was injected from the left at the position $z = 1.35$ m with a total current of 75 A. After passing the retarding potential the beam hits the collector wall with a total remaining power of 2.2 MW. Fig. 3 shows particle trajectories for the case where no sweeping is applied. The resulting peak power density exceeds 2500 W/cm^2.

In our first simulations of the sweeping system we ignored the effects of eddy currents in the copper walls
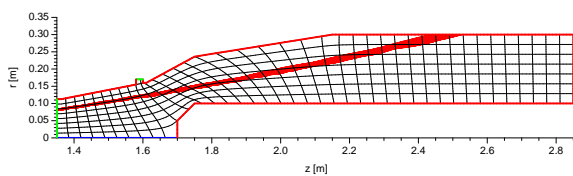
Figure 3: Particle trajectories in the case of zero collector coil current.
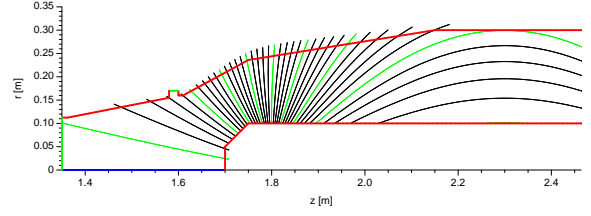
Figure 4: Magnetic field lines created by the collector solenoids without the influence of copper walls.
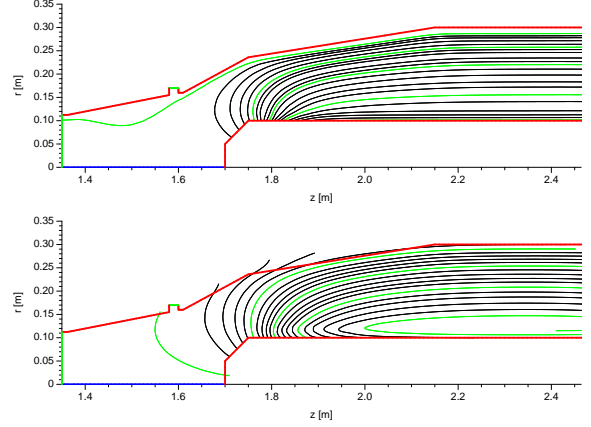
Figure 5: Magnetic field lines created by the collector solenoids with the influence of eddy currents in the copper walls for $f_{\mathrm{sweep}} = 10$ Hz (top: real part, bottom: imaginary part).

of the collector. The magnetic field lines of the collector solenoids only are shown in Fig. 4. By modulating the collector coil current with a sinusoidal time dependence in the range $I_{\mathrm{sweep}} = -30$ A $\ldots$ $+10$ A one obtains a sweeping area with a length of approximately 70 cm. The resulting averaged power density on the collector wall is shown in Fig. 6 (top) and indicates a peak power density below 450 W/cm^2. This value is well acceptable from the technical point of view.

However, since the planned thickness of the outer wall is 12 mm, the effect of eddy currents can not be ignored. With the help of the ANSYS FEM software the magnetic field distributions in the collector region has been calculated taking into acount the influence of eddy currents in the metallic collector walls. The resulting field lines (real and imaginary parts) are shown in Fig. 5 for a sweeping frequency of 10 Hz. Since the magnetic field experiences a phase shift with respect to the applied coil current one obtains a complex solution for the magnetic field $\vec{B}_{\mathrm{FEM}}$. The value of the field at time t can be calculated with

$$\vec{B}(z,r,t) = \Re(\vec{B}_{\mathrm{FEM}}(z,r)e^{i\omega t}),$$

where $\omega/2\pi = f_{\mathrm{sweep}}$ is the frequency of the applied coil current.

Using these realistic magnetic fields we had to realize that due to the effect of eddy currents the sweeping region along the collector wall reduces to values below

No copper, $I_{\mathrm{sweep}} = -30\,\mathrm{A} \,...\, +10\,\mathrm{A}$

$f_{\mathrm{sweep}} = 3\,\mathrm{Hz}, \quad I_{\mathrm{sweep}} = -40\,\mathrm{A} \,...\, +20\,\mathrm{A}$

$f_{\mathrm{sweep}} = 10\,\mathrm{Hz}, \quad I_{\mathrm{sweep}} = -40\,\mathrm{A} \,...\, +20\,\mathrm{A}$
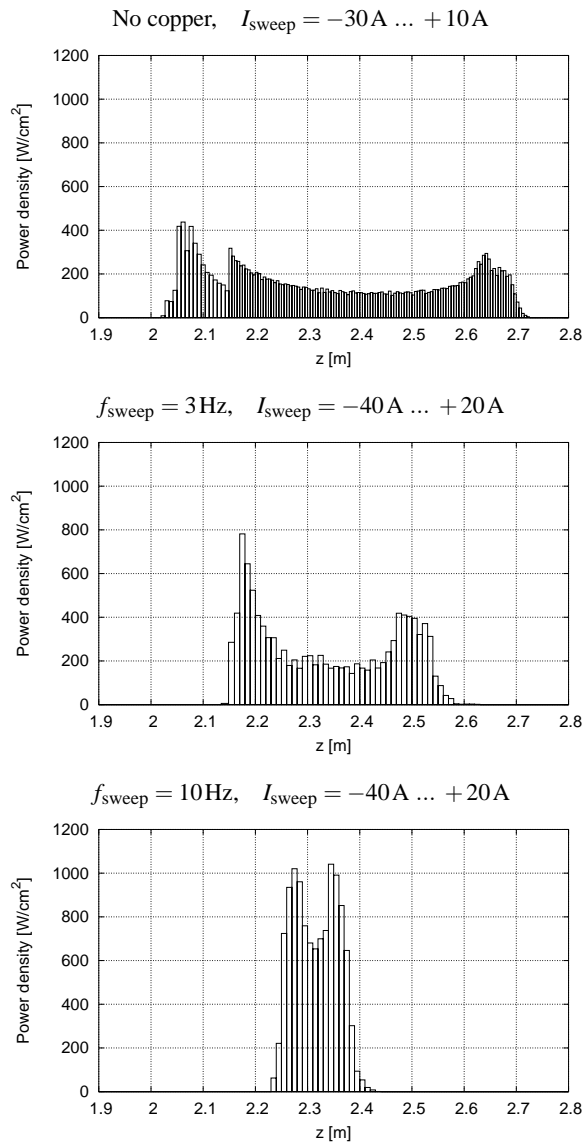
Figure 6: Distribution of the averaged power density on the collector wall. Top: without influence of copper walls; middle and bottom: with influence of copper walls at sweeping frequencies of 3 Hz and 10 Hz.

20 cm at $f_{\mathrm{sweep}} = 10\,\mathrm{Hz}$. Even an increase of the coil current by 50% did not help significantly. The resulting power density distribution is plotted in Fig. 6 (bottom) and shows an unacceptable high peak power density of about $1000\,\mathrm{W/cm^2}$. Even at an unrealistic low sweeping frequency of only 3 Hz one obtains a peak power density close to $800\,\mathrm{W/cm^2}$ (c.f. Fig. 6, middle).

4   Conclusion and outlook

With the originally suggested collector design with sweeping coils placed inside the hollow electron beam a good distribution of the beam power along the collector surface has been obtained in calculations if the effect of eddy currents in the collector walls has been ignored. In addition, a fast sweeping frequency (up to 50 Hz) seemed to be possible because there is only low power dissipation on the wall surrounding the sweeping coils and therefore a thickness of only about 4 mm copper can be taken. Due to the influence of the eddy currents mainly in the outer collector wall with a thickness of about 12 mm the distribution of the sweeping field is strongly modified already for frequencies above a few Hz. This modified field distribution results in a strong reduction of the sweeping range and thus in an unacceptable increase of the power loading on the collector wall. As a consequence a new design is under investigation. A collector coil inserted within the beam will be used for generation of a static magnetic field which varies along the beam path sufficiently fast as needed for non-adiabatic motion. Due to this the radial width of the electron beam will be broadened resulting in a reduction of the instantaneous peak power density. Additionally a slow sweeping with $f_{\mathrm{sweep}} \leq 10\,\mathrm{Hz}$ will be performed with coils placed outside the collector as is used in conventional high power gyrotrons.

There is no power loading due to the primary beam at the insert inside the collector. Secondary electrons in particular of higher generation may hit the insert and cause some loading. With the modified trajectory code this loading will be calculated.

References

[1] H. Zohm, et al., "Experiments on neoclassical tearing mode stabilization by ECCD in ASDEX Upgrade" Nuclear Fusion, vol. 39, pp. 577-580, 1999

[2] G. Dammertz, S. Alberti, A. Arnold, E. Borie, V. Erckmann, et al., "Development of a 140 GHz, 1 MW, 140 GHz, Continuous Wave Gyrotron for the W7-X Stellarator", IEEE Trans. Plasma Sci., vol. 30, no. 3, pp. 808-818, 2002

[3] T. Imai, N. Kobayashi, R. Temkin, M. Thumm, M.Q. Tran, V. Alikaev, "ITER R&D: Auxiliary Systems: Electron Cyclotron Heating and Current Drive System", Fusion Engineering and Design, 55, pp. 281-289, 2001

[4] B. Piosczyk, A. Arnold, G. Dammertz, O. Dumbrajs, M. Kuntze, M. Thumm, "Coaxial cavity gyrotrons — recent experimental results", IEEE Trans. Plasma Sci., vol. 30, No. 3, pp. 819-827, 2002

[5] M.A. Leontovitch, Ed., Reviews of Plasma Physics. New York: Consultants Bureau, 1965, vol. 1.

[6] G.B. Collins, "Microwave Magnetrons", Chapter 12, McGraw Hill, 1948